Fluorescent Mesoporous Nanoparticles for β-Lactamase Screening Assays

Srikrishna Tummala,[a] Wei-An Huang,[a] Bo-Hong Wu,[a] Kai-Chih Chang,*[b] and Yen-Peng Ho*[a]

We present a sensitive and rapid screening method for the determination of β-lactamase activity of antibiotic-resistant bacteria, by designing a pH-sensitive fluorescent dye-doped mesoporous silica nanoparticle encapsulated with penicillin G as a substrate. When penicillin G was hydrolysed by β-lactamase and converted into penicilloic acid, the acidic environment resulted in fluorescence quenching of the dye. The dye-doped mesoporous nanoparticles not only enhanced the β-lactamase-catalyzed reaction rate but also stablized the substrate, penicillin G, which degrades into penicilloic acid in a water solution without β-lactamase. Twentyfive clinical bacterial samples were tested and the antibiotic resistant and susceptible strains were identified. The proposed method may detect the presence of β -lactamases of clinically relevant samples in less than 1 hour. Moreover, the detection limit of β-lactamase activity was as low as 7.8×10^{-4} U/mL, which was determined within two hours.

1. Introduction

The emergence of antibiotic-resistant bacteria has become a major concern to the public health, which is due to the misuse and over usage of antibiotics. The World Health Organization (WHO) has listed bacterial resistance as one of the human health crises. Thus, there is a need to quickly and accurately identify the antibiotic-resistance of bacteria. β-Lactam antibiotics are the widely used antibacterial agents over the past decades. After the discovery of penicillin, a number of modifications were developed for different therapeutic effects.[1] β-lactam antibiotics may hinder the bacterial cell wall synthesis and render the cell wall vulnerable to environmental osmotic pressure, leading to the cell rupture.[2] One of the most common antibiotic-resistant mechanisms is the production of β-lactamases. The β-lactamase is an enzyme that may hydrolyse a β-lactam ring of antibiotics and reduce the antibacterial activity of drugs.[3] Determination of antibiotic-resistance of bacteria should be rapid, easy, and quantitative.

Earlier studies demonstrate several methods to identify antibiotic-resistant bacteria, which include antimicrobial susceptibility test (AST), E-test, disk diffusion and broth dilution. The major drawback of these methods is time-consuming. In general, it takes 24 to 48 h to obtain test results.[4] In the past decade, sensing antibiotic-resistant bacteria has been achieved by using a number of assays such as iodometric assay,[5] acidimetric assay,[6] and chromophoric assay.[7] Advanced methods have been reported, such as electrochemical biosensing,[8] PCR,[9] and mass spectrometric detection.[10] In addition to the above methods, many fluorescence-based assays have been reported using fluorogenic substrates of β-lactamases.[11,12] The substrates are lactams modified with moieties of fluorophores or quenchers and fluorophores. Reaction of the substrates with the lactamase may lead to a turn-on or turn-off of the fluorescence. A fluorescent probe for lactamase has been developed by combining a DNA aptamer and a graphene oxide nanomaterial. The aptamer modified with a fluorophore was attached to the graphene oxide material and the sensing was realized through the FRET mechanism.[13] However, the gene-based methods may detect only the genes of known sequence and many fluorescence methods require complicated synthesis techniques.

Silica nanoparticle has a wild range of applications in bio-nanotechnology due to their physical, chemical, and optical properties such as chemical modification diversity, biocompatibility, optical transparency, low toxicity, and particle-size tunability.[14] Silica nanoparticles are mostly used in drug delivery,[15] biosensors,[16] and bio-imaging.[17] Mesoporous silica nanoparticles (MSNPs) own a unique structure with an adjustable pore and particle size, leading to a large specific surface area which can be easily functionalized. Furthermore, the large surface area and pore volume ensure facile loading of various target/substrate materials. Dye-doped silica nanoparticles exhibit bright and stable fluorescence[18] and may play an important role in the aforementioned biological applications. Several strategies have been reported to synthesize the luminescent porous silica nanoparticles. One strategy is to embed the dye into the silica matrix during particle formation. Another approach is to add the dye after the porous structure has formed.

In this work, we developed a sensitive and rapid fluorescent assay for detecting β-lactamase in antibiotic-resistant bacteria by

[a] S. Tummala, W.-A. Huang, B.-H. Wu, Prof. Y.-P. Ho
Department of Chemistry, National Dong Hwa University, Hualien, 974 Taiwan, (Republic of China)
E-mail: ypho@gms.ndhu.edu.tw

[b] Prof. K.-C. Chang
Department of Laboratory Medicine and Biotechnology, Tzu Chi University, Hualien, 970 Taiwan, (Republic of China)
E-mail: kaichih@mail.tcu.edu.tw

ChemistryOpen

Full Papers
doi.org/10.1002/open.202000221

Chemistry Europe
European Chemical
Societies Publishing

designing fluorescent mesoporous nanoparticles (FMSNPs). The water-soluble fluorescent molecules (fluorescein isothiocyanate, FITC) with high quantum yield[19] were incorporated onto the particle surface by chemical reaction. Then, the substrate (penicillin G, PenG) of β-lactamase was loaded onto the fluorescent mesoporous particles. When the substrate reacted with β-lactamase, penicilloic acid was produced and the decrease in the pH of the environment caused fluorescence quenching of the particles. Clinical samples of antibiotic-resistant and -susceptible strains were studied to demonstrate the feasibility of the approach.

2. Results and Discussion

2.1. Characterization of the Synthesized FMSNP/PenG

The morphology and structure of synthesized FMSNPs were investigated by SEM, TEM, Brunauer-Emmett-Teller (BET), XRD, zeta potential and FT-IR analysis. As shown in Figure 1a, the particles have a uniform spherical shape with an average diameter of 86 nm. The TEM image shown in Figure 1b indicates an average pore size of 2 nm in diameter. The pore size is consistent with the value (2.083 nm) determined by the BET curve measurement shown in Figure 1c. The small angle XRD patterns (Figure 1d) of pure MSNPs show (100), (110), and (200) reflections at 2θ of 2.21, 3.72 and 4.24, respectively, which is characteristic of a hexagonal structure.[20] On other hand, the peak intensities were decreased gradually after the particles were modified with FITC and PenG (Figure 1d, inset), indicating a reduction in mesoporous ordering.[21] As shown in Figure S1, the surface modifications of

MSNPs were confirmed by the zeta potential measurements. The pure MSNPs were negatively charged with the zeta potential of −11.1 mV due to the deprotonation of the surface silanol groups (Si−OH). After the APTES and FITC were covalently bound to the surface groups of MSNPs, the zeta potential was increased to a positive value (10.2 mV). Further encapsulation with PenG did not change the zeta potential (9.84 mV). The PenG was attached to the particle presumably through hydrogen bonding between the carboxylic group on PenG and the functional groups on the particles, causing no significant change in charge of the modified particles. Although the zeta potential was not very high, the size distribution of the synthesized FMSNP/PenG remained very stable after 24 h (Figure S2), indicating that no aggregation occurred. The FT-IR spectra (Figure S3) were also employed to confirm the structures of MSNP, FITC, FMSNP, PenG and the composite of PenG and FMSNP (FMSNP/PenG). The IR peaks of MSNP at 471.6 cm^{-1}, 809.1 cm^{-1}, and 1110.4 cm^{-1} correspond to O−Si−O bending, symmetric stretching (broad), and asymmetric stretching vibrations, respectively. The peak at 1246.2 cm^{-1} is assigned to NH (NH$_2$) stretching and the signal at 3434.7 cm^{-1} is due to OH stretching. The peaks of pure FITC was observed at 1587.7 cm^{-1} from benzene ring stretching, 2024.1 cm^{-1} from −N=C=S stretching, and ~2800 cm^{-1} from CH stretching. The peaks of synthesized FMSNPs revealed C−O−C stretching at 961.0 cm^{-1}, C=C stretching at 1476.9 cm^{-1}, and C=O stretching at 1638.1 cm^{-1}. The disappearance of the peak at 2024.1 cm^{-1} (−N=C=S stretching) indicated that covalent bond was formed between −N=C=S on FITC and -NH$_2$ on silica nanoparticles. The bands for pure PenG at 780–690 cm^{-1}, 1550 cm^{-1}, 1690 cm^{-1}, and 1760 cm^{-1} were assigned to skeletal vibrations of aromatic ring, amide (II) stretching, amide C=O stretching, and β-lactam C=O stretching, respectively. The FT-
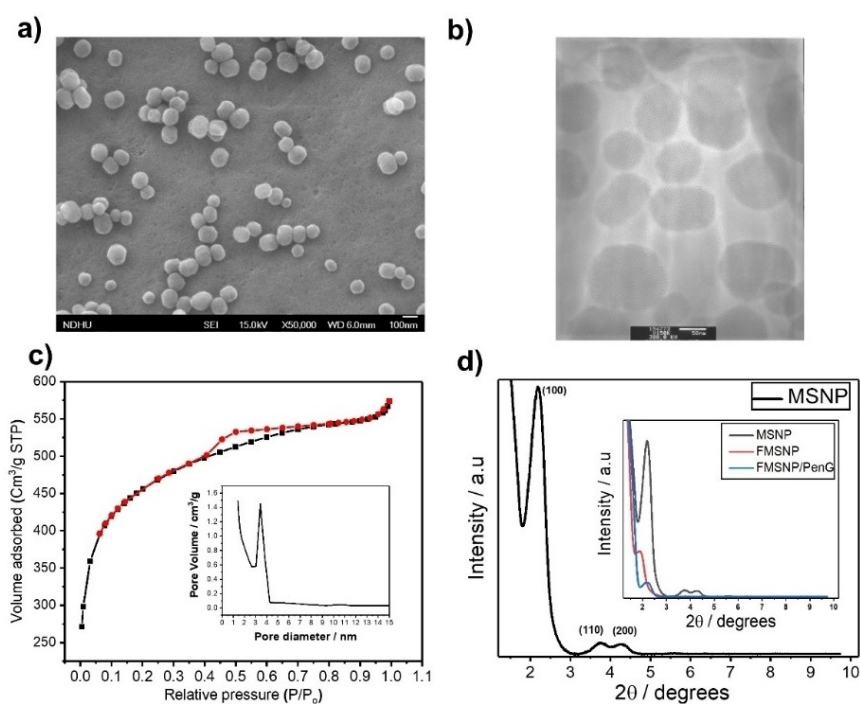

Figure 1. Characterization of FMSNP/PenG: (a) SEM micrograph, (b) TEM micrograph, (c) BET curve, (d) Small angle XRD patterns (Figure 1d) of pure MSNP. Inset: the change in peak intensities after the particles (MSNP) were modified with FITC (FMSNP) and PenG (FMSNP/PenG).

ChemistryOpen

Full Papers
doi.org/10.1002/open.202000221

Chemistry Europe
European Chemical
Societies Publishing

IR spectrum of FMSNP/PenG showed peaks at 780–690 cm^{-1} from skeletal aromatic vibrations, 961.0 cm^{-1} from C–O–C stretching, 809.1–1110 cm^{-1} from Si–O–Si symmetric stretching, 1638.1 cm^{-1} from C=O stretching, 1760 cm^{-1} from β-lactam C=O stretching, and 3434.7 cm^{-1} from OH stretching. These results indicated that the PenG was indeed loaded into FMSNP.

## 2.2. β-Lactam Antibiotic Resistance Detection Using FMSNP/PenG

When the FITC dye-doped nanoparticles containing PenG (FMSNP/PenG) are incubated in a solution of β-lactamase, the β-lactamase cleaves the β-lactam ring of PenG and converts PenG into penicilloic acid. The fluorescent FITC is a pH sensitive dye and converted to a non-fluorescent structure under an acidic condition with a pH value less than 5.5 (Scheme 1).[22] Therefore, when the β-lactamase secreted from resistant bacteria interacts with FMSNP/PenG, the fluorescence of the particles is quenched. The catalytic reaction may produce sufficient penicilloic acid to quench the fluorescence with a small amount of β-lactamase enzyme present in the samples.

Figure 2a shows the fluorescence spectra of dye-doped nanoparticles at various pH values between 3.3 and 8.2 and under excitation at 490 nm. Decrease of one pH unit from 7 to 6 caused an obvious decrease of fluorescence intensity. Further decrease to pH 5.2 reduced the fluorescence to 23.7% of that at pH 7.1 based on the peak area. The significant fluorescence quenching could be detected by naked eyes using a hand-held UV lamp with an excitation wavelength at 365 nm (Figure 2a, inset panel). The rate of pH change arising from β-lactamase catalysis depends on the concentration of penicillin G. Figure 2b shows the pH changes for the catalytic reaction of 5 units of β-lactamase with aqueous penicillin G at different concentrations (10 mg/10 mL, 25 mg/10 mL, 50 mg/10 mL, and 100 mg/10 mL). The reaction reached completion in about 3 hours. Moreover, penicillin G at a concentration of 10 mg/10 mL could only reduce the pH value of the aqueous solution to 5.4. If the concentration of penicillin G was raised to 25 mg/10 mL, 50 mg/10 mL and 100 mg/10 mL, the pH of the solution was reduced to about 4.3 and no significant decrease in pH of the solution after 24 h of reaction. In antibiotic resistance experiments, the PenG concentration at ca. 50 mg/10 mL was chosen to provide ample amount of substrate to reduce the pH of the reaction solutions. The approach for the detection of antibiotic resistance is based on the hydrolysis of penicillin G by lactamase, leading the decrease of pH in solutions and the quenching of fluorescence from FITC. One may argue that
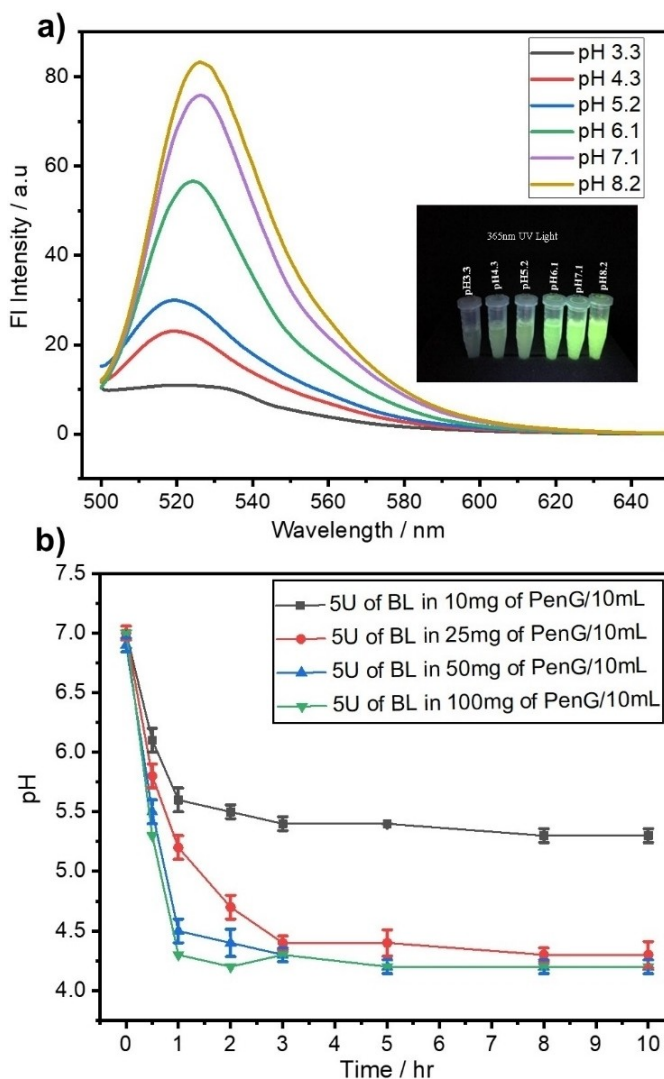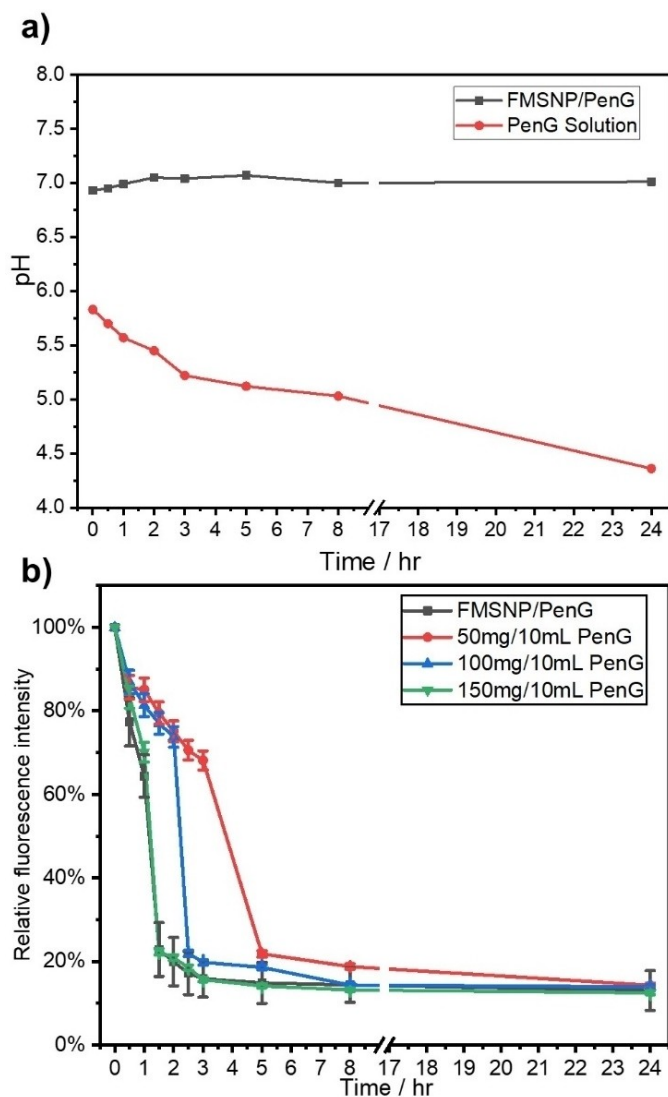

Figure 2. (a) Fluorescence spectra of FMSNPs (490 nm irradiation) at different pH values. The inset panel shows the photo of FMSNP samples at various pH conditions under a hand-held UV lamp (365 nm irradiation). (b) Time plot of pH values for the reaction of β-lactamase (5 units) with the substrate (PenG) at various concentrations (10 mg/10 mL, 25 mg/10 mL, 50 mg/10 mL, and 100 mg/10 mL).

the use of free-form penicillin G may serve the same purpose. Figure 3a shows the time plot of pH change in the aqueous solution of free-form penicillin G or in the suspension of penicillin G immobilized on mesoporous particles. The free penicillin G is acidic in nature. The pH of the prepared solution was 5.8. Further, we noted that the compound degraded gradually in solution even
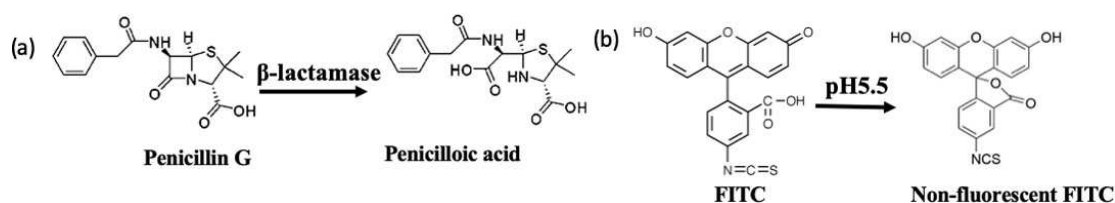
Scheme 1. (a) The catalysis of penicillin G by β-lactamase and (b) the structure change of fluorescein isothiocyanate (FITC) under acidic conditions.

ChemistryOpen

Full Papers
doi.org/10.1002/open.202000221

Chemistry Europe
European Chemical
Societies Publishing

Figure 3. (a) Time plot of pH changes in the aqueous solution of free-form penicillin G or in the suspension of PenG-immobilized mesoporous particles. (b) The rate of fluorescence change for the β-lactamase assay (0.05 U/mL) with and without the nanoparticles.

without the catalysis of lactamase, leading to a pH as low as 4.3. The acidic nature renders the fluorescence approach impossible. However, when the penicillin G was loaded onto FMSNPs, the pH remains extremely stable at arround 7. The carboxlic group on penicillin G may involve in the interaction between the penicillin G and the silicate/amino groups on particles presumably through hydrogen bonding. This interaction will stabilize the proton on carboxlic group and result in a stable neutral solution. The reults indicate that penicillin-immobilized particles are essential to the sucess of this approach. The immobilized particles will ensure that any fluorescence quenching was arising only from the pH change caused by the β-lactamase. The percentage of PenG in FMSNP/PenG catalyzed by β-lactamase was estimated based on the concentration of penicilloic acid produced during the catalysis. The total concentration of the penicilloic acid was determined through the acid dissociation constant (pKa = 2.29) and the pH
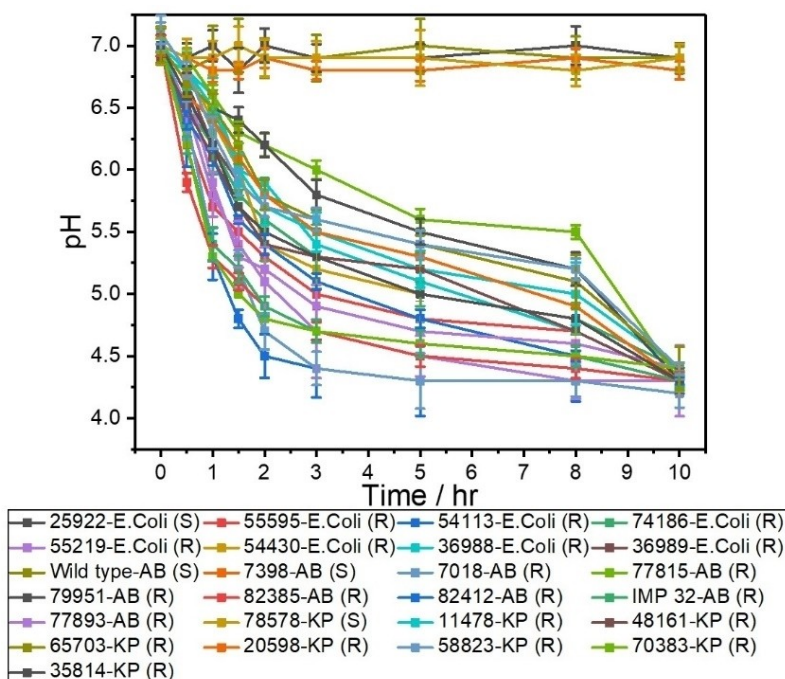
measurement of the reaction. The percentage of PenG in FMSNP/PenG catalyzed by β-lactamase (0.5 U/mL) was 0.48% after 12 h reaction (Table S1). The low percentage might be attributed to the relatively large amount of FMSNP/PenG used and the intrinsic enzymatic characteristics. However, the pH change was good enough to trigger the fluorescence quenching.

The penicillin G-loaded mesoporous nanoparticles also enhanced the reaction rate. Figure 3b compares the β-lactamase assay (0.05 U/mL) with and without the nanoparticles. The fluorescence vs time plot of the catalytic reaction in the FMSNP/PenG suspension was compared to those in the PenG solutions at 50 mg/10 mL, 100 mg/10 mL and 150 mg/10 mL. The FITC concentration in the PenG solution was 32 µM. The absorbance of the FITC dye at the concentration of 32 µM is equivalent to that in the FMSNP/PenG suspension. The amount of FMSNPs (56.2 mg) loaded with PenG was used so that the total amount of doped PenG is equivalent to that of PenG in 50 mg/10 mL of the free-form PenG solution. When the amount of enzyme substrate (PenG) in the solution (50 mg/10 mL) is equivalent to that in the particle suspension, the reaction for the free solution is much slower than for the particle suspension. The reaction rate for the free solution became similar to that for the particle suspension when the substrate solution is increased three times to 150 mg/mL. The results indicate that enzymatic reaction is more efficient in the nanoparticle system. It is because that the local concentration of PenG was higher in mesoporous particles than in the free solution, therefore, the enzymatic reaction rate was enhanced.

2.3. Analysis of Clinical Bacterial Samples Using the FMSNP/PenG Approach

The tested clinical samples include 25 strains of three bacterial species (*Acinetobacter baumannii* (AB), *Klebisella pnenumoniae* (KP), *Escherichia coli* (*E. coli*)). The bacterial samples were mixed with FMSNP/PenG. The change in pH value of the suspension was measured as a function of incubation times (Figure 4). A stable pH value was observed through incubation time for four bacterial samples including two strains of *A. baumannii*, one strain of *E. coli*, and one strain of *K. pnenumoniae*. All of these strains were determined to be antibiotic-susceptible by a conventional method. The other 21 strains showed various extent of pH change over incubation times. The difference among the 21 samples reflected that these clinical species contain various lactamase activities.

Figure 5a shows the relative fluorescence intensities of the FMSNP/PenG suspension mixed with various concentrations of β-lactamase solution having activities ranging from 0.5 to 0.00078 unit/mL. The fluorescence decreased quickly to 20% in 1 hour when the activity was 0.5 unit/mL. It took 8 hours for the fluorescence to decrease to 23% when the β-lactamase activity was 0.00078 unit/mL. Overall, the rate for the fluorescence change is increased with the increase of β-lactamase activity. Table 1 lists the relative fluorescence intensity versus reaction times. When the reaction was carried out without β-lactamase (0 unit/mL), the fluorescence remained very stable (99%) even after 24 hours of reaction. All the relative intensities were decreased to detectable level around 75% in 1hr as long as the activity of β-lactamase was

ChemistryOpen

Full Papers
doi.org/10.1002/open.202000221

Chemistry Europe
European Chemical
Societies Publishing

Figure 4. The change in pH value of the suspension was measured as a function of incubation times. The figure legend indicates bacterial species *Acinetobacter baumannii* (AB), *Klebisella pnenumoniae* (KP), *Escherichia coli* (*E.coli*) with resistance (R) or suceptibility (S) to antibiotics.
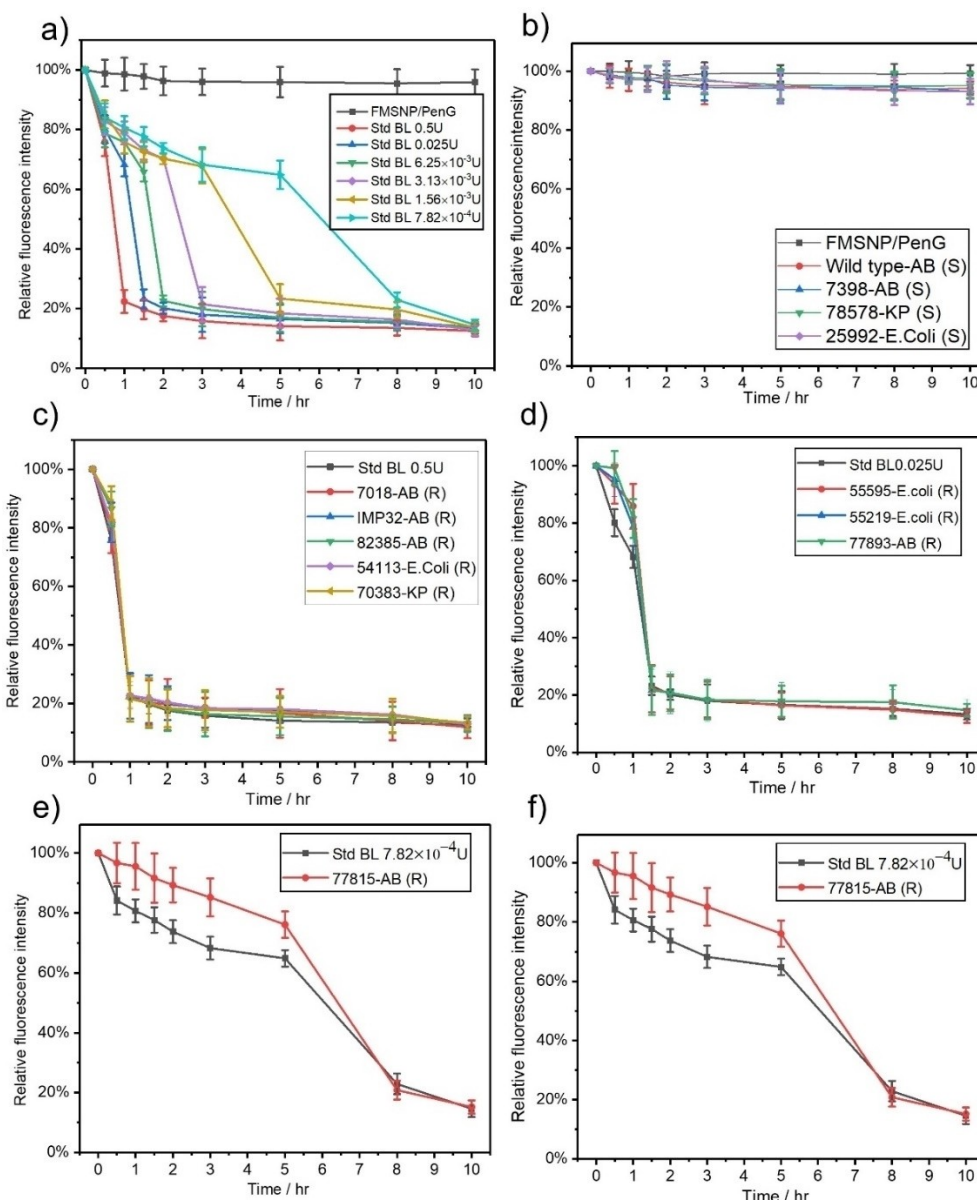
Table 1. Relative fluorescence intensity vs reaction time for the FMSNP/PenG suspension in response to the different activity of β-lactamase.

Reaction time (hr) BL activity (U/mL)	0	0.5	1	1.5	2	3	5	8	24
	Relative fluorescence intensity (%)								
0	100	99.8±0.8	99.3±0.4	99.1±1.2	98.9±0.7	99.1±0.8	99.2±1.2	99.0±1.7	99.2±0.7
0.5	100	74.3±6.2	19.4±4.2	15.7±3.1	14.9±3.2	14.4±2.5	13.5±3.4	13.1±1.8	12.4±0.5
0.25	100	80.9±5.3	23.8±2.6	19.8±3.6	18.1±3.3	17.4±2.1	16.0±2.4	15.4±2.3	13.3±1.3
0.1	100	76.1±7.2	24.2±3.4	21.0±2.5	18.2±5.3	17.3±3.1	14.3±4.7	13.9±2.8	12.9±1.7
0.05	100	78.5±6.8	71.5±3.9	24.2±5.2	22.3±6.5	20.7±4.5	18.8±5.6	17.3±3.8	12.2±2.2
0.025	100	80.7±6.5	73.2±3.8	23.4±5.4	21.7±6.2	21.0±4.3	19.2±5.4	18.1±13.7	15.3±3.2
0.0125	100	81.6±8.4	76.6±5.3	73.3±4.7	22.7±3.6	21.3±6.2	20.3±5.1	19.8±4.2	16.7±3.1
0.00625	100	79.2±6.3	77.0±5.4	74.7±4.7	65.6±3.6	24.7±6.1	21.5±5.3	18.1±3.4	14.0±2.3
0.003125	100	82.9±5.7	78.9±6.2	73.2±5.7	70.3±5.6	21.4±4.9	18.4±6.1	16.3±4.2	12.8±2.3
0.001563	100	85.1±5.3	75.9±5.0	72.6±3.2	70.3±6.1	67.7±4.2	23.4±3.7	19.7±3.5	13.7±2.7
0.000782	100	84.1±5.8	80.7±4.2	77.6±3.7	73.7±5.2	68.3±6.1	64.9±3.6	22.9±3.8	14.6±2.1

higher than 0.025 unit/mL. The relative fluorescence intensity was 80% and 74% at a reaction time of 1 h and 2 h, respectively, even when the activity of lactamase was as low as 7.82×10^{-4} unit/mL. Based on the standard deviation of all the measurements (three replicates) listed in Table 1, the maximum relative standard deviation of the FMSNP/PenG approach is 10%. Therefore, the decrease of fluorescence by 25% should be significant. To the best of our knowledge, this is the lowest detected activity ever reported. The method may be employed to quickly screen the antibiotic-resistance in less than two hours.

Figure 5b shows the fluorescence vs time plot for the reaction of FSNP/PenG with antibiotic-susceptible bacterial strains. These antibiotic-susceptible bacteria do not produce β-lactamase that may quench the fluorescence of FSNP/PenG. Thus, the fluorescence intensity of suspension remained unchanged over the reaction time. The fluorescence intensities were compared

between two FSNP/PenG suspensions containing the β-lactamase standard and 21 clinical specimens, respectively. Figures 5c–f display the match in fluorescence intensity between some bacterial samples and the β-lactamase standard with known activities. The FSNP/PenG approach not only identifies the presence of β-lactamase in bacteria but also gives estimated activities of the β-lactamase using the matching plots. All of the 21 samples gave reasonable matches to β-lactamase standards of certain activities. We note that the *A. baumannii* 77815 strain was tested susceptible using a nitrocefin disk method.[23] This strain was found to be antibiotic-resistant with lactamase activity near 7.8×10^{-4} unit/mL (Figure 5f) using the proposed approach. The antibiotic resistance was further confirmed by a PCR method. The result indicates that the proposed method is very sensitive and might avoid false negatives.

ChemistryOpen

Full Papers
doi.org/10.1002/open.202000221

Chemistry Europe
European Chemical
Societies Publishing

Figure 5. (a) Fluorescence vs time plot for the reaction of FSNP/PenG with β-lactamase standard of various activities. (b) Fluorescence vs time plot for the reaction of FSNP/PenG with antibiotic-susceptible bacterial strains. Comparison of the fluorescence intensities between two FSNP/PenG suspensions containing respectively the clinical bacterial strains and the β-lactamase standard with varying activities of (c) 0.5 U/mL, (d) 0.025 U/mL, (e) 6.25×10^{-3} U/mL, and (f) 7.82×10^{-4} U/mL. The figure legend indicates bacterial species *Acinetobacter baumannii* (AB), *Klebisella pnenumoniae* (KP), *Escherichia coli* (*E.coli*) with resistance (R) or suceptibility (S) to antibiotics.
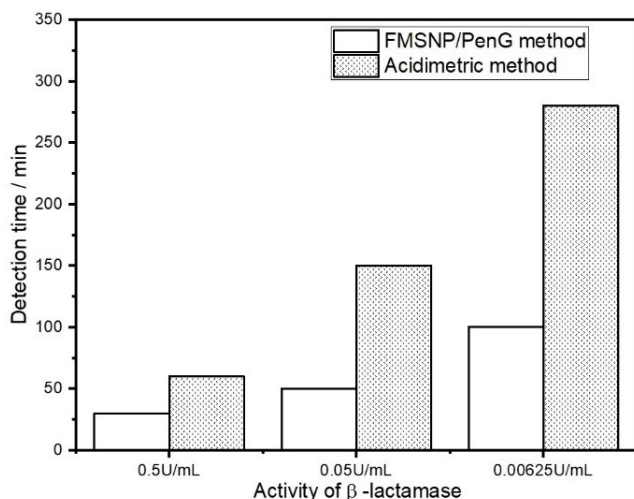
2.3.1. Comparing the FMSNP/PenG approach with the traditional acidimetric method

The acidimetric method has been used to detect the presence of β-lactamase based on a pH-dependent color change. We also performed the aciditimeteric test using a phenol red reagent and recorded the time for the color change from purple to yellow at certain β-lactamase acitivities. Figure 6 compares the detection time between the acidimetric method and the FMSNP/PenG approach. The detection time of the present method is defined as the time required to reduce the relative fluorescence intensity to less than 75%. The reaction times were 30 min and 60 min for the present method and the acidimetric method, respetively, when

the activity of β-lactamase was 0.5 U/mL. The reaction time for the present method was 100 min and for the acidimetric was 280 min when the activity of β-lactamase was 0.00625 U/mL. The present method is significantly faster (two to three times) than that of the acidimetric method at the equivalent concentrations of β-lactamase.

3. Conclusions

We have established a sensitive and rapid approach for the detection of β-lactamase present in antibiotic-resistant bacteria.

ChemistryOpen

Full Papers
doi.org/10.1002/open.202000221

Chemistry Europe
European Chemical
Societies Publishing

Figure 6. Comparison of the detection time between the proposed method and the acidimetric assay at different activities of β-lactamase.

The approach employed a pH-sensitive fluorescent dye-doped mesoporous silica nanoparticle encapsulated with a β-lactamase substrate, penicillin G. The mesoporous nanoparticles plays an essential role in the detection process by stablizing the substract and enhancing the β-lactamase-catalyzed reaction rate. The method has been successfully applied to the analysis of 25 clinical bacterial strains. Future work will involve extending the method to other substrates and biological applications.

Experimental section

Materials and Chemicals

Cetyl trimethyl ammonium bromide (CTAB), tetraethyl orthosilicate (TEOS), 3-aminopropyltriethoxysilane (APTES), penicillin G, fluorescein isothiocyanate, and β-lactamase from *Enterobacter cloacae* (type IV, lyophilized powder, 0.2–0.6 units/mg protein) were purchased from Sigma-Aldrich (St. Louis, Mo, USA). Phenol red was purchased from Alfa Aesar (Tewksbury, Ma, USA). Clinical bacteria samples were obtained from Dr. Kai-Chi Chang's lab at Tzu Chi University.

Instruments

Fluorescence measurements were recorded with an FP-750 Spectrofluorometer (Jasco, Tokyo, Japan). The size and morphology of mesoporous silica nanoparticles were determined using a field emission scanning electron microscope (SEM, Model JSM-7500F, JEOL, Japan) operated at an accelerating voltage of 15 kV. The pore size and morphology of the mesoporous nanoparticles were verified by an analytical transmission electron microscope (TEM, Model JEM-3010, JEOL, Japan) operated at 300 kV. UV-Vis absorption spectra were recorded using a UV-Vis spectrophotometer (model U-3900, Hitachi, Japan). The X-ray deffraction (XRD) patterns of mesoporous silica nanoparticles were recorded on an XRD instrument (Brukers, D2 phaser 2nd generation Xe.T) equipped with a Cu Kα source ($\lambda = 1.54$ Å). The surface charges of mesoporous particles were recorded by a Zetasizer Nano-ZS (Malvern Instru-

ments, Malvern, UK). The functional groups of mesoporous nanoparticles were identified using a Fourier transform infrared spectrometer (Spectrum One, perkinElmer, USA) in the wavenumber range from 4000 cm^{-1} to 400 cm^{-1}.

Preparation of Fluorescent Dye-Doped Mesoporous Silica Nanoparticles *(FMSNPs)*

Sodium hydroxide (2 M, 0.35 mL) was added to 0.1 g of CTAB in 50 mL water and heated up to 70 °C under stirring. Then, TEOS and APTES (0.5 mL each) were added to the solution. One minute later, 0.5 mL of ethyl acetate was added and the reaction was carried out at 70 °C for 24 hours with stirring. The synthesized silica nanoparticles were collected by centrifugation at 10,000 rpm for 20 minutes and washed four times with DI water and ethanol, respectively. Then, silica nanoparticles were extracted with ethanol by reflux for 6 hours to remove CTAB and the mesoporous silica nanoparticles were collected. The FITC dye (4 mg) was mixed with 44 mL of APTES and 1 mL of ethanol under stirring in the dark room for 24 hours. The particles were mixed with 50 μL of the prepared dye solution and 100 mL of ethanol and heated under reflux at pH 11 for 12 hours. The 530-nm fluorescence of the dye-doped particle suspension was measured under excitation at 490 nm.

Loading of Penicillin G Into FMSNPs

The synthesized fluorescent mesoporous silica nanoparticles (56.2 mg) were mixed with an aqueous solution of penicillin G (210 mg/30 mL) and the mixture was shaken overnight. Then, the particles were collected by centrifugation and washed with DI water to remove loose penicillin from the surface of mesoporous nanoparticles. The supernatants were collected and the amount of penicillin G was measured by a UV spectrometer. The UV absorption of the PenG solution before and after the loading assay was 0.885 and 0.695, respectively. The amount of antibiotics loaded into the FMSNPs was calculated by substracting the amount of penicillin G left in the supernatant from the total amount of the starting material. One milligram of FMSNPs was estimated to contain 0.89 mg of penicillin G. The nanoparticles were freeze-dried and stored at 4 °C. To compare the stability of penicillin G in an aqueous solution and in a FMSNP/PenG suspension, the pH values of the FMSNP/PenG suspension (56.2 mg FMSNP/10 mL) and the penicillin G solution (50.0 mg/10 mL) were monitored under shaking at various times. To measure the percentage of PenG in FMSNP/PenG catalyzed by β-lactamase, 2 mg of FMSNPs loaded with PenG was mixed with 0.5 U of β-lactamase in 1 mL at room temperature. The pH values were measured at various reaction times and used to determine the total concentration of penicilloic acid produced during the catalysis period. The mole number of catalyzed PenG was assumed to be equal to that of penicilloic acid produced.

Analysis of Clinical Bacterial Samples Using FMSNPs

Clinical bacterial isolates were cultured one day before the β-lactamase analysis. Briefly, single colony of each bacterium was inoculated in LB liquid medium and incubated at 37 °C with gentle shaking for 12 hours. The bacterial samples were diluted with LB broth and the final concentration of 10^9 CFU/mL was obtained by spectrophotometric measurement of O.D. at 600 nm. The suspension was centrifuged at 2100 rpm for 5 min, followed by washing three times to remove supernatant and resuspending in DI water for further use.

ChemistryOpen

Full Papers
doi.org/10.1002/open.202000221

Chemistry Europe
European Chemical
Societies Publishing

The bacterial sample (10^9 CFU/mL, 1 mL) and 56.2 mg of FMSNPs loaded with PenG were mixed and diluted to 10 mL with DI water. The mixture was shaken in a mixer and 1 mL of the suspension was drawn at given times for the measurement of pH and fluorescence. All the errors indicated in pH and fluorescence plots were standard deviations determined from three replicates.

Acidimetric Test

The testing solution was prepared by adding 200 μL of 1% phenol red to 1800 μL of aqueous solution containing 10 mg of penicillin G. The solution was adjusted to pH 8.5 with 1 N sodium hydroxide and became dark purple. The solution was mixed with various concentrations of β-lactamase. The final solution was shaken and the time when the solution turned yellow (pH 6) was recorded.

Conflict of Interest

The authors declare no conflict of interest.

[1] N. Kardos, A. L. Demain, *Appl. Microbiol. Biotechnol.* **2011**, *92*, 677.

[2] a) J. F. Fisher, S. O. Meroueh, S. Mobashery, *Chem. Rev.* **2005**, *105*, 395–424; b) K.-F. Kong, L. Schneper, K. Mathee, *APMIS* **2010**, *118*, 1–36; c) C. Walsh, *Nature* **2000**, *406*, 775; d) M. S. Wilke, A. L. Lovering, N. C. J. Strynadka, *Curr. Opin. Microbiol.* **2005**, *8*, 525–533.

[3] a) X.-Z. Li, M. Mehrotra, S. Ghimire, L. Adewoye, *Vet. Microbiol.* **2007**, *121*, 197–214; b) D. M. Livermore, *Clin. Microbiol. Rev.* **1995**, *8*, 557–584; c) J. R. Knowles, *Acc. Chem. Res.* **1985**, *18*, 97–104.

[4] a) J. Rello, *Eur. Respir. Rev.* **2007**, *16*, 33–39; b) D. L. Paterson, *Clin. Infect. Dis.* **2006**, *42*, S90–S95; c) G. P. Wormser, M. M. Bergman, *Clin. Infect. Dis.* **2003**, *36*, 238–238; d) J. Deasy, *J. Am. Acad. Phys. Assist.* **2009**, *22*, 18–22; e) T. Huang, Y. Zheng, Y. Yan, L. Yang, Y. Yao, J. Zheng, L. Wu, X. Wang, Y. Chen, J. Xing, X. Yan, *Biosens. Bioelectron.* **2016**, *80*, 323–330.

[5] a) C. Man, X. Pang, K. Xie, Y. Lu, S. Liu, S. Yang, Y. Liu, Y. Jiang, *Int. Dairy J.* **2013**, *33*, 44–48; b) M. G. Sargent, *J. Bacteriol.* **1968**, *95*, 1493–1494; c) T. Sawai, I. Takahashi, S. Yamagishi, *Antimicrob. Agents Chemother.* **1978**, *13*, 910–913; d) R. P. Novick, *Biochem. J.* **1962**, *83*, 236–240; e) N. Zyk, *Antimicrob. Agents Chemother.* **1972**, *2*, 356–359.

[6] a) F. A. Rubin, D. H. Smith, *Antimicrob. Agents Chemother.* **1973**, *3*, 68–73; b) L. Roger, A. Jane, L. G. Francois, *FEBS Lett.* **1973**, *33*, 42–44; c) E. Anago, L. Ayi-Fanou, C. D. Akpovi, W. B. Hounkpe, M. Agassounon-Djikpo Tchibozo, H. S. Bankole, A. Sanni, *Ann. Clin. Microbiol. Antimicrob.* **2015**, *14*, 5; d) B. B. Wintermans, C. M. J. E. Vandenbroucke-Grauls, *J. Microbiol. Methods* **2016**, *120*, 29–33.

[7] a) C. H. O'Callaghan, A. Morris, S. M. Kirby, A. H. Shingler, *Antimicrob. Agents Chemother.* **1972**, *1*, 283–288; b) R. N. Jones, H. W. Wilson, W. J. Novick, *J. Clin. Microbiol.* **1982**, *15*, 677–683; c) B. Chantemesse, L. Betelli, S. Solanas, F. Vienney, L. Bollache, A. Hartmann, M. Rochelet, *Water Res.* **2017**, *109*, 375–381; d) S. Lee, S. Kang, M. S. Eom, M. S. Han, *Dyes Pigm.* **2017**, *137*, 518–522.

[8] T. M. d Prado, M. V. Foguel, L. M. Gonçalves, M. d P T Sotomayor, *Sens. Actuators B* **2015**, *210*, 254–258.

[9] Z. Liu, J. Zhang, S. Rao, L. Sun, J. Zhang, R. Liu, G. Zheng, X. Ma, S. Hou, X. Zhuang, X. Song, Q. Li, *J. Microbiol. Methods* **2015**, *110*, 1–6.

[10] a) Z. Xu, H.-Y. Wang, S.-X. Huang, Y.-L. Wei, S.-J. Yao, Y.-L. Guo, *Anal. Chem.* **2010**, *82*, 2113–2118; b) L. N. Ikryannikova, E. A. Shitikov, D. G. Zhivankova, E. N. Il'ina, M. V. Edelstein, V. M. Govorun, *J. Microbiol. Methods* **2008**, *75*, 385–391.

[11] a) W. Gao, B. Xing, R. Y. Tsien, J. Rao, *J. Am. Chem. Soc.* **2003**, *125*, 11146–11147; b) B. Xing, A. Khanamiryan, J. Rao, *J. Am. Chem. Soc.* **2005**, *127*, 4158–4159; c) T. Naqvi, R. Singh, *Mol. BioSyst.* **2007**, *3*, 431–438; d) Y. Chen, Y. Xianyu, J. Wu, W. Zheng, J. Rao, X. Jiang, *Anal. Chem.* **2016**, *88*, 5605–5609; e) M. Wuyu, X. Lingying, W. Yaqun, X. Hexin, *Chem. Asian J.* **2016**, *11*, 3493–3497; f) H. B. D. Thai, J. K. Yu, B. S. Park, Y.-J. Park, S.-J. Min, D.-R. Ahn, *Biosens. Bioelectron.* **2016**, *77*, 1026–1031; g) C. M. June, R. M. Vaughan, L. S. Ulberg, R. A. Bonomo, L. A. Witucki, D. A. Leonard, *Anal. Biochem.* **2014**, *463*, 70–74; h) Z. Lan, C. Wing-Lam, C. Wai-Hong, L. Yun-Chung, W. Kwok-Yin, C. Pak-Ho, *Chem. Eur. J.* **2010**, *16*, 13367–13371; i) S. Khan, U. W. Sallum, X. Zheng, G. J. Nau, T. Hasan, *BMC Microbiol.* **2014**, *14*, 84; j) J. Aw, F. Widjaja, Y. Ding, J. Mu, Y. Liang, B. Xing, *Chem. Commun.* **2017**, *53*, 3330–3333; k) X. Zheng, U. W. Sallum, S. SarikaVerma, H. Athar, C. L. Evans, T. Hasan, *Angew. Chem. Int. Ed.* **2009**, *48*, 2148–2151; l) S. Yu, A. Vosbeek, K. Corbella, J. Severson, J. Schesser, L. D. Sutton, *Anal. Biochem.* **2012**, *428*, 96–98.

[12] L. Peng, L. Xiao, Y. Ding, Y. Xiang, A. Tong, *J. Mater. Chem. B* **2018**, *6*, 3922–3926.

[13] J. Qin, X. Cui, P. Wu, Z. Jiang, Y. Chen, R. Yang, Q. Hu, Y. Sun, S. Zhao, *Food Control* **2017**, *73*, 726–733.

[14] J. E. Lee, N. Lee, T. Kim, J. Kim, T. Hyeon, *Acc. Chem. Res.* **2011**, *44*, 893–902.

[15] A. Watermann, J. Brieger, *Nanomaterials* **2017**, *7*, 189.

[16] M. Hasanzadeh, N. Shadjou, M. de la Guardia, M. Eskandani, P. Sheikhzadeh, *TrAC Trends Anal. Chem.* **2012**, *33*, 117–129.

[17] F. Peng, Y. Su, Y. Zhong, C. Fan, S.-T. Lee, Y. He, *Acc. Chem. Res.* **2014**, *47*, 612–623.

[18] a) A. Burns, H. Ow, U. Wiesner, *Chem. Soc. Rev.* **2006**, *35*, 1028–1042; b) S. Veeranarayanan, A. Cheruvathoor Poulose, S. Mohamed, A. Aravind, Y. Nagaoka, Y. Yoshida, T. Maekawa, D. S. Kumar, *J. Fluoresc.* **2012**, *22*, 537–548.

[19] M. L. Vera, A. Cánneva, C. Huck-Iriart, F. G. Requejo, M. C. Gonzalez, M. L. Dell'Arciprete, A. Calvo, *J. Colloid Interface Sci.* **2017**, *496*, 456–464.

[20] J. S. Beck, J. C. Vartuli, W. J. Roth, M. E. Leonowicz, C. T. Kresge, K. D. Schmitt, C. T. W. Chu, D. H. Olson, E. W. Sheppard, S. B. McCullen, J. B. Higgins, J. L. Schlenker, *J. Am. Chem. Soc.* **1992**, *114*, 10834–10843.

[21] Y. Gao, S. L. Zhong, L. F. Xu, S. H. He, Y. M. Dou, S. N. Zhao, P. Chen, X. J. Cui, *Microporous Mesoporous Mater.* **2019**, *278*, 130–137.

[22] a) J. Xu, L. Sun, J. Li, J. Liang, H. Zhang, W. Yang, *Nanoscale Res. Lett.* **2011**, *6*, 561; b) J. Xu, J. Liang, J. Li, W. Yang, *Langmuir* **2010**, *26*, 15722–15725; c) S. Yao, K. J. Schafer-Hales, K. D. Belfield, *Org. Lett.* **2007**, *9*, 5645–5648.

[23] T. T. Jiang, R. R. Liu, X. F. Huang, H. J. Feng, W. L. Teo, B. G. Xing, *Chem. Commun.* **2009**, 1972–1974.